An Originally Developed Centrifuge Test Apparatus for Simulating Tunnel Structure Crossings at Arbitrary Active Fault Angles

Guanxiong ZENG
Department of Civil and Earth Resources Engineering, Kyoto University, Kyoto, Japan,
zeng.guanxiong.7c@kyoto-u.ac.jp

Yasuhito KAMOI, Yasuo SAWAMURA, Kiyoshi KISHIDA
Department of Urban Management, Kyoto University, Kyoto, Japan, *kamoi.yasuhito.78z@st.kyoto-u.ac.jp, sawamura.yasuo.6c@kyoto-u.ac.jp, kishida.kiyoshi.3r@kyoto-u.ac.jp*

ABSTRACT: Linear underground infrastructures, such as tunnel structures, inevitably traverse active fault zones, where fault displacements during seismic events can cause severe structural damage and significant economic losses. To investigate the mechanical behaviour of tunnels intersecting active faults, this study introduces an originally developed centrifuge apparatus designed to simulate tunnel-fault interactions. The apparatus features an L-shaped movable frame that represents the hanging wall of the active fault. This frame is driven by both horizontal and vertical jacks, whose displacement rates are manually controlled to replicate reverse or normal fault displacements at arbitrary dip angles. Notably, this setup incorporates a fault-plane guider, which ensures that the fault dip angle is consistently maintained from the bottom to the ground surface, thereby enabling a direct intersection between the tunnel model and the fault plane. The experiments are conducted using the centrifuge modelling system at the Disaster Prevention Research Institute (DPRI), Kyoto University, under a centrifugal acceleration field of 50g. The ground is modelled with Toyoura sand, and the tunnel structure is simulated using an aluminium pipe. A total of 48 strain gauges are installed on the tunnel to capture its structural response, while 16 earth pressure sensors are deployed to monitor soil-tunnel interaction during fault displacement. A series of centrifuge tests were carried out to examine the mechanical responses of tunnels subjected to both reverse and normal fault displacements. The experimental findings provide valuable insights into tunnel behaviour under active fault displacement and offer important references for future design and analysis.

1 INTRODUCTION

Active fault displacement during seismic events has induced severe damage to linear underground structures like transportation tunnels, pipelines, water supply systems, etc. (Lawson et al., 1908; Asakura et al., 2000; Konagai et al., 2003; Chen et al., 2023).

Relative to theoretical or numerical approaches, model experiments are viewed as offering more realistic insights into the mechanical behavior and damage characteristics of linear underground structures affected by active fault displacement. Centrifuge model tests are capable of reproducing the mechanical response of large-scale structures with relatively small model dimensions while replicating the effects of the in-situ stress field. Therefore, they have been widely adopted in geotechnical research (Iai et. Al., 2005, Ueda et al., 2019).

The previous research set the loading systems under the soil and let the fault plane to generate automatically during loading (Burridge et al., 1989; Tohidifar et al., 2019; Cai et al., 2019; Sabagh & Ghalandarzadeh, 2020; Yao et al., 2021). This results in that the research subjects of the existing studies are the tunnels or underground structures passing over the active fault but not those directly intersect with the active fault (Fig. 1). Hence the results gained from the existing research could not sufficiently serve as the reference of the current study about the tunnel directly crosses the active fault.

Meanwhile, many previous studies revealed that the tunnel responses under fault displacement vary with different tunnel-fault intersecting angles (Liu et al., 2015; Zeng et al., 2024) and fault types including reverse or normal faults (Ghadimi & Tahghighi, 2019; Qiao et al., 2022). But no existing research revealed these differences.

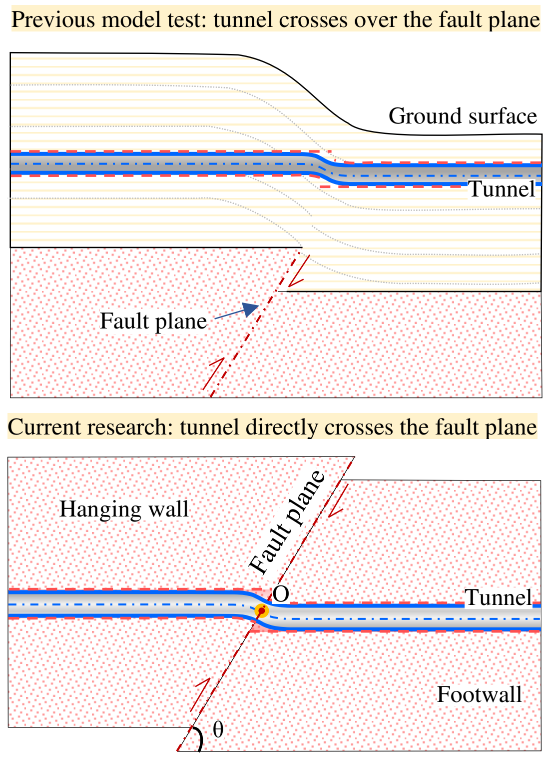

Figure 1. The position connection of the tunnel and active fault in previous and current research.

It is necessary to create or establish a brand-new experiment apparatus to fulfil these gaps. This paper introduces an originally designed apparatus for researching the active fault crossing tunnel structure under different tunnel-fautl intersecting angles and fault types.

2 EXPERIMENTAL APPARATUS

2.1 Overall dimensions and components

The overview of the experimental apparatus used in this study is shown in Fig. 2. The experimental apparatus consists of an aluminum rigid soil container with dimensions of 690 mm (length, x direction) × 400 mm (width, z direction) × 535 mm (height, y direction). Inside this container, there is a soil box of 500 mm (length) × 300 mm (width) × 350 mm (height).

As discussed before, this apparatus is designed for simulating a tunnel directly crosses an active fault. For this purpose, a fault-plane guider is introduced to simulate the generation of the fault plane. This fault-plane guider holds a dip-angle of θ, which could be changed to adjust the generated fault dip-angle.

The soil box is divided by this fault-plane guider in the x direction into two sides: the Hangwall side and the Footwall side. The boundaries of Footwall side stay stable during the experiment. While the boundaries of the Hanging wall side are composed of an L-shaped movable frame. This L-shaped movable frame is connected with the jack systems, which assigns manually controled displacement during the experiment.

There are two larser displacement sensors to detect the vertical and horizontal displacement of this L-shaped movable frame during the experiment.

To allow the L-shaped movable frame to move during the experiment, small gaps existed between the apparatus's walls and the movable frame, To prevent the leakage of the sandy soil, an L shaped cover (Fig.2) and a membrane cover (Fig.4) were installed.

To allow visual observation of the soil behavior during the experiment, the front face is made of high strength glass.

2.2 Loading systems

The loading systems of this apparatus is composed by four jack systems, two for vertical loading and 2 for horizontal loading.

Both the horizontal and vertical loading systems consist of two jack systems. The motor in each jack system holds a torque capacity of 37 kN·m (Oriental Motor Co., ARM98AC-PS36).

The components of the horizontal jack system, for instance, is shown in Fig.3. There is a motor which controls the rotational speed of a shaft, and the shaft moves a rectangular block vertically along it. This block is connected to two triangular prisms, which transform its vertical displacement into horizontal displacement, subsequently appling to the L-shaped movable frame.

2.2.1 Reverse fault displacement

During the experiment, the L-shaped movable frame was displaced both horizontally and vertically to simulate fault displacements within the sandy soil. To simulate a reverse fault, the L-shaped movable frame was displaced upward in the vertical direction and displaced rightward in the horizontal direction.

The maximum vertical displacement of the L-shaped movable frame when simulating reverse fault displacement is set as 16mm (80cm in prototype), with a loading speed of 0.5mm/min. The horizontal displacement of the L-shaped movable frame is adjusted according to the fault dip-angle θ, obeying the following equation:

$$U = {}^{V}\!/_{\tan(\theta)} \qquad (1)$$

where U refers to the horizontal displacement, mm; V refers to the vertical displacement, mm.

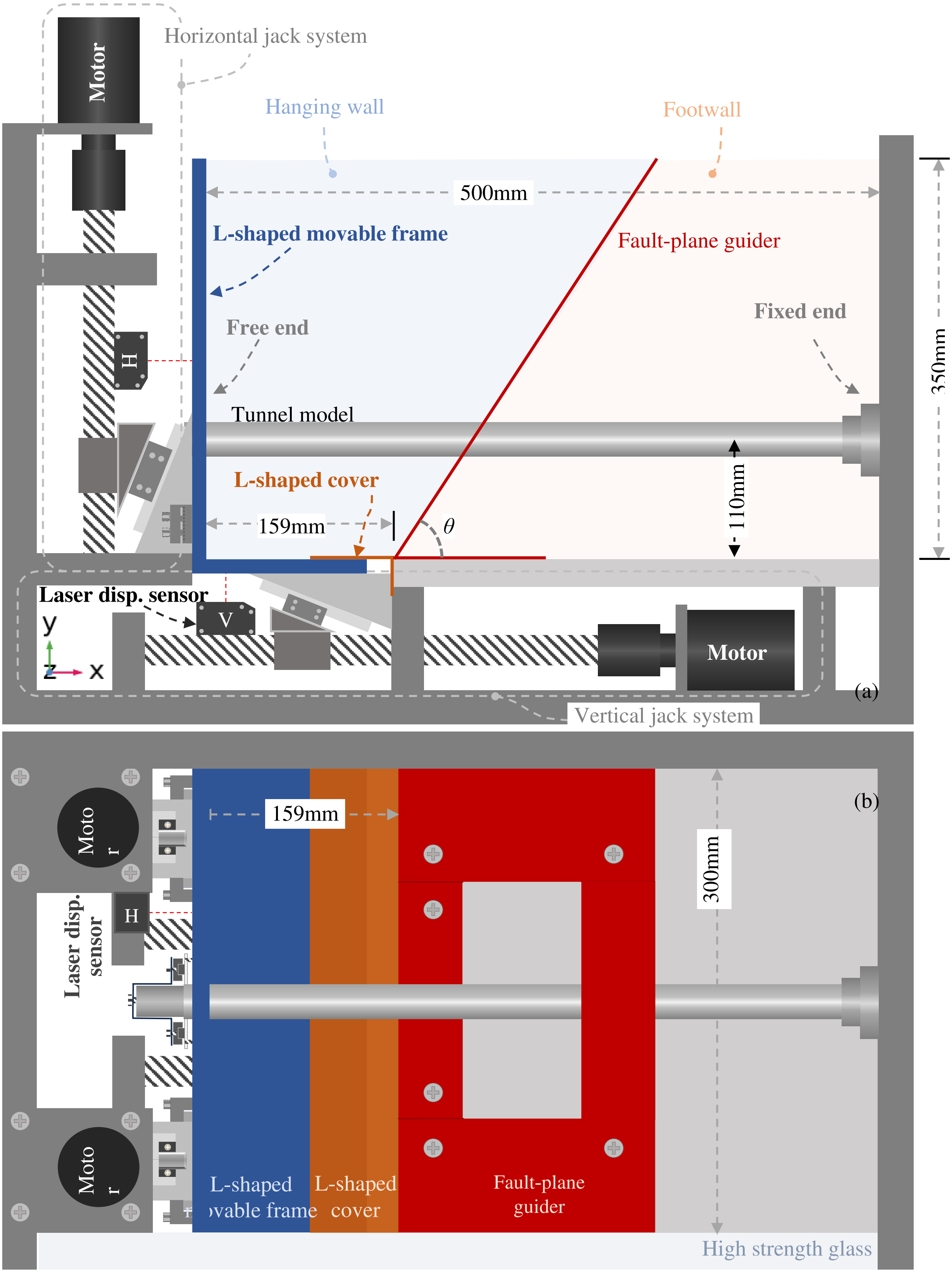

Figure 2. The geometry and scheme of the experimental apparatus: (a) front view; (b) vertical view.

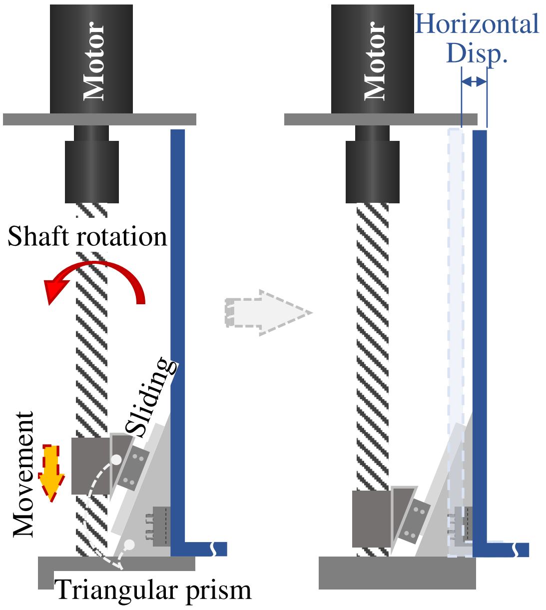

Figure 3. The displacement of the horizontal jack system.

2.2.2 Normal fault displacement

For simulating normal fault displacement, the apparatus should supply tensile loading in both horizontal and vertical directions.

The gravity during centrifuge model test could supply the tensile loading in the vertical direction. To supply the tensile loading in the horizontal direction, a special device (Fig.4) is designed and installed to connect the horizontal jack system and the L-shaped movable frame. Therefore, the tensile loading could be transferred to the L-shaped movable frame when the horizontal jack system moves backward.

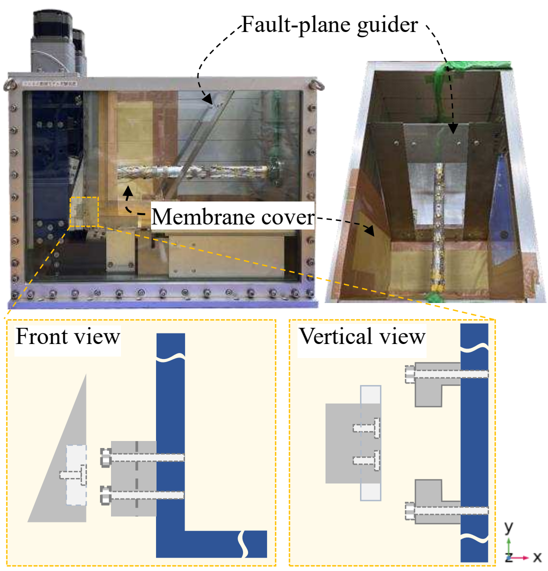

Figure 4. The experimental apparatus, the fault plane guider and the horizontal loading system.

The maximum vertical displacement of the L-shaped movable frame when simulating normal fault displacement is set as -16mm (negative direction of *y* axial), with a loading speed of 0.5mm/min. The horizontal displacement of the L-shaped movable frame also obeys equation (1).

2.3 Tunnel model and the measuring points

The tunnel is simulated by pipe made of aluminium (A6063TE-T5, Fig.5), holding diameter of 30mm, thickness of 1mm and length of 508mm. The elastic modulus of aluminium alloy is 70GPa. The tunnel model is located at 110mm in the *y* direction (Fig.2) and at the middle of the apparatus in the *z* direction (Fig.4).

The aluminium alloy is selected for the model tunnel lining because its mechanical behavior is approximately linear-elastic and isotropic, which minimizes material-induced nonlinearity in the test results and facilitates direct comparison with analytical and numerical models. However, the elastic modulus of aluminum is substantially higher than that of prototype linings, which may introduce stiffness-scale mismatch and affect the measured response.

Strain gauges were attached to the tunnel model to record the strain of the structure during faulting (Fig.5). For the aluminum pipe, strain gauges type FLAB-03-23-2LHT-F (Tokyo Measuring Instruments Laboratory) which is specifically for metal was used.

As shown in Fig.5, there are 12 slices of strain gauges in total and the strain of 4 positions were measured in each slice: A, B, O and O`. Positions A and B are the upper and lower side of the tunnel, respectively. While positions O and O` are in the middle of the tunnel. The strain gauges attached in position O measure the deformation of the cross-section of the tunnel. While the strain gauges attached in the other positions are measuring the tunnel deformation in the longitudinal direction.

Earth pressure sensors (PDA-PB, Tokyo Measuring Instruments Laboratory) were also attached to the tunnel model to measure the soil-tunnel interaction during faulting. The earth pressure sensors are only attached to the Line A and B, for 7 positions on each line. The positions of the earth pressure sensors are in the middle of nearby strain gauges.

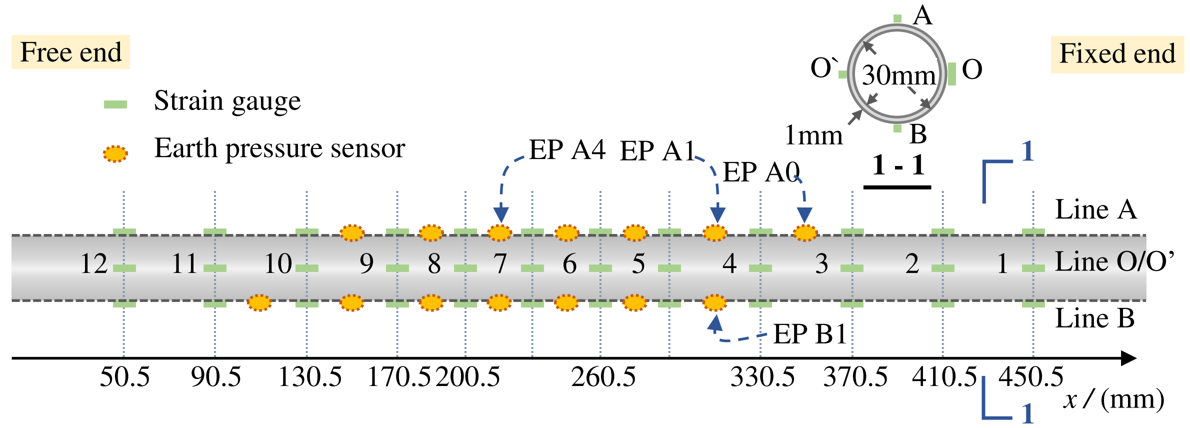

Figure 5. Distribution of the measurement points under reverse fault displacement.

Notably, according to the soil-tunnel interaction patterns revealed in Zeng et al., (2024), under reverse faulting conditions, the fault-induced earth pressure in the hanging wall acts on the lower part of the tunnel, while that in the footwall acts on the upper part. Accordingly, the earth pressure sensors on the upper side of the tunnel (Line A) were installed near the fixed end—closer to the footwall—covering the range from x = 150.5 mm to 350.5 mm. The earth pressure sensors on the lower side (Line B) were placed near the free end—closer to the hanging wall—in the range of x = 110.5 mm to 310.5 mm.

2.4 Boundary condition

To prevent the tunnel model from shifting during the experiment, one end was kept free while the other was fixed to the wall as a fixed end.

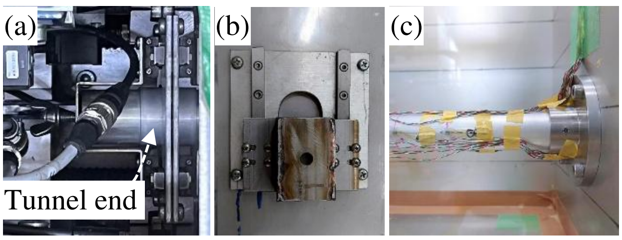

Figure 6. Boundary conditions of the tunnel model: (a) the free end (vertical view) and (b) the free end (front view); (c) the fixed end.

The free end was inserted into a vertical displacement guide rail on the L-shaped movable frame, as illustrated in Fig.6(a) and (b), allowing it to move freely in both vertical and horizontal direction.

The fixed end of the tunnel model is fixed onto the sidewall of the apparatus (Fig.6(c)).

2.5 Model ground

In this experiment, Toyoura sand was used as ground material. The physical properties of Toyoura sand are listed in Table 1. The model ground was prepared with a relative density of 80% using the tamping method.

The height of the ground is 300mm, dividing into 5 layers. The first layer from the surface is 44mm while the other 4 layers hold a height of 64mm. To visually track the ground displacement, the colored sand, blue-colored silica sand with a particle size of 0.425–0.600 mm, was used to create 2 mm-deep colored sand layers between two layers.

Table 1. The physical properties of Toyoura sand (Tsutsumi et al., 2006).

Physical properties	Values
Specific gravity of soil particles	2.66
Mean particle diameter / mm	0.21
Internal friction angle / deg	40.6
Cohesion / kPa	0
Maximum void ratio	0.992
Minimum void ratio	0.632
Unit weight / kN/m³	15.41

3 EXPERIMENT RESULTS

This experiment was conducted using the centrifuge loading device owned by the Disaster Prevention Research Institute (DPRI), Kyoto University, under a centrifugal acceleration field of 50G.

To obtain the vertical displacement of the bending tunnel structure, double integration is required. First, the curvature is derived from the strain distribution that measured from Line A and B and then integrated twice to yield the vertical displacement. During the integration, the rotation angle and the vertical displacement of the tunnel at the fixed-end (x=500mm) is set as 0 to determine the integration constant.

The longitudinal stresses of Line A and B are derived by multiplying the detected strain and elastic modulus of aluminium, i.e., 70GPa.

3.1 Assigned fault displacement

Experiments are conducted to reveal the mechanical responses of tunnel structure under the displacement of 60° reverse and normal fault.

Fig.7(a) shows the vertical and horizontal displacement assigned to the L-shaped movable frame, which is identical to the 60° reference line. Fig.7(b) shows the front view of soil box after the experiment. The trace of the fault plane is clearly depicted by the layers of colored sand. This trace is identical to the 60° reference line

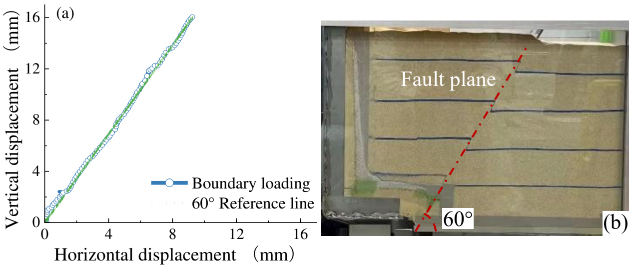

Figure 7. Fault displacement: (a) displacement assigned to the L-shaped movable frame; (b) front view of soil box after the experiment.

3.2 Tunnel deformation under 60° reverse fault displacement

The vertical displacement of tunnel under 60° reverse fault displacement is shown in Fig.8(a), which shows typical S-shaped bending deformation under reverse fault displacement.

The longitudinal stresses of Line A and B are shown in Fig.8(b). The upper part of the tunnel, Line A, is under tension in the Haning wall side and under compression in the footwall side. While the lower part of the tunnel, Line B, is under compression on the Hanging wall side and under tension on the footwall side.

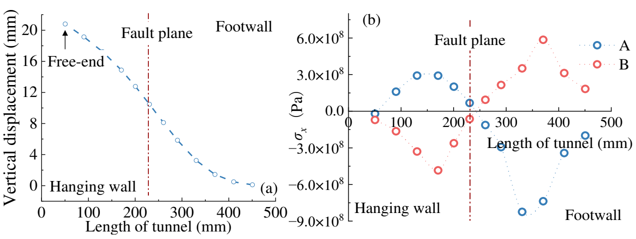

Figure 8. Longitudinal tunnel responses under 60° reverse fault displacement: (a) vertical displacement of tunnel; (b) stress distribution of Lines A and B.

3.3 Tunnel deformation under 60° normal fault displacement

The vertical displacement of tunnel under 60° normal fault displacement is shown in Fig.9(a). Instead of the typical S-shaped deformation discussed before, the tunnel shows a V-shaped deformation. Meanwhile, the longitudinal distribution of stress in Fig.9(b) also shows that the upper part of the tunnel is under tension while the lower part of the tunnel is under compression. This pattern again proves the V-shaped deformation.

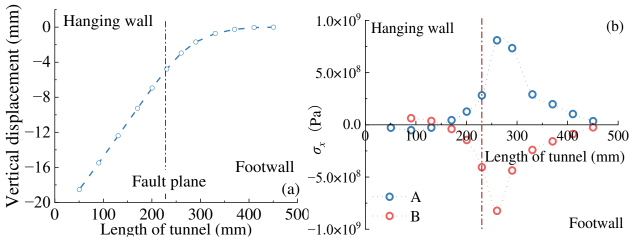

Figure 9. Longitudinal tunnel responses under 60° normal fault displacement: (a) vertical displacement of tunnel; (b) stress distribution of Lines A and B.

Because of the dimensional constraints of centrifuge loading device in DPRI, the model length in this study is relatively limited and one end of the tunnel is treated as free. Consequently, the results can be regarded as indicative of the mechanical behavior of the portal section of a tunnel subjected to normal fault displacement.

4 CONCLUSIONS

This paper originally developed an apparatus to research the mechanical responses of an active fault crossing tunnel structure under reverse or normal fault displacement. The conclusions can be drawn as follows:

(1) An apparatus for simulating tunnel structure directly crosses an active fault is originally developed. By controlling the displacement rates of horizontal and vertical jacks, this apparatus can replicate reverse or normal fault displacements at arbitrary dip angles. A fault-plane guider maintains a consistent fault orientation, allowing accurate modelling of tunnel-fault intersections.

(2) Two centrifuge model experiments were conducted to research the mechanical responses of tunnel structure under reverse or normal fault displacement. The results verified the “S-shaped” deformation of tunnel structure under faulting. Meanwhile, it shows that a “V-shaped “deformation may be induced to tunnel structure, when the active

normal crosses a short tunnel with light overburden like the culvert or intersects a tunnel near its portal.

The elastic modulus of aluminum alloy considerably exceeds that of prototype linings, potentially causing a stiffness-scale discrepancy that can bias test responses. Consequently, subsequent experiments will use acrylic (PMMA), whose lower elastic modulus mitigates this mismatch and may yield behavior more representative of the prototype.

ACKNOWLEDGEMENTS

This work was supported by JSPS KAKENHI Grant Number 23KK0076 and Takahashi Industrial and Economic Research Foundation.

REFERENCES

Asakura, T., Shiba, Y. Matsuoka, S., Oya, T. and Yashiro K., 2000. Damage to mountain tunnels by earthquake and its mechanism, Doboku Gakkai Ronbunshu, No. 659/III-52, 27-38.

Burridge, P. B., Scott, R. F., & Hall, J. F., (1989). Centrifuge study of faulting effects on tunnel. Journal of geotechnical engineering, 115(7), 949-967.

Cai, Q. P., Peng, J. M., Ng, C. W., Shi, J. W., & Chen, X. X., (2019). Centrifuge and numerical modelling of tunnel intersected by normal fault rupture in sand. Computers and Geotechnics, 111, 137-146.

Chen, P., Geng, P., Chen, J., & Gu, W., (2023). The seismic damage mechanism of Daliang Tunnel by fault dislocation during the 2022 Menyuan Ms6. 9 Earthquake based on unidirectional velocity pulse input. Engineering Failure Analysis, 107047.

Ghadimi Chermahini, A., & Tahghighi, H., (2019). Numerical finite element analysis of underground tunnel crossing an active reverse fault: a case study on the Sabzkouh segmental tunnel. Geomechanics and Geoengineering, 14(3), 155-166.

Iai, S., Tobita, T., & Nakahara, T., (2005). Generalised scaling relations for dynamic centrifuge tests. Geotechnique, 55(5), 355-362.

Konagai K., Hori M., Meguro K., Matsushima T, & Yamaguchi Y., 2003. Control of failure modes of civil-infrastructures experiencing large soil deformations caused by surface fault ruptures, Re-port of research project 2000 Grant-in-Aid for Scientific Research (A) (No. 12355020) Japan So-ciety for the Promotion of Science.

Lawson, A. C., & Harry F. R., 1908. The California earthquake of April 18, 1906: Report of the state earthquake investigation commission... No. 87. Carnegie Institution of Washington.

Liu, X., Li, X., Sang, Y., & Lin, L., (2015). Experimental study on normal fault rupture propagation in loose strata and its impact on mountain tunnels. Tunnelling and Underground Space Technology, 49, 417-425.

Qiao, Y., Tang, J., Liu, G., & He, M., (2022). Longitudinal mechanical response of tunnels under active normal faulting. Underground Space, 7(4), 662-679.

Sabagh, M., & Ghalandarzadeh, A., (2020). Numerical modelings of continuous shallow tunnels subject to reverse faulting and its verification through a centrifuge. Computers and Geotechnics, 128, 103813.

Tohidifar, H., Moosavi, M., & Jafari, M. K., (2019). Behavior of Tunnels against the Reverse Faulting Deformations Using Centrifuge Test and Numerical Modelling. Journal of Seismology & Earthquake Engineering, 21(2).

Tsutsumi, Y., Sato, T., & Koseki, J., (2006). Dynamic and static measurements of small strain moduli of dry Toyoura sand. Seisan-Kenkyu; *Journal of Institute of Industrial Science*, The University of Tokyo, 58(6), 521-524. (in Japanese)

Ueda, K., Sawada, K., Wada, T., Tobita, T., & Iai, S., (2019). Applicability of the generalized scaling law to a pile-inclined ground system subject to liquefaction-induced lateral spreading. Soils and Foundations, 59(5), 1260-1279.

Yao, C., He, C., Takemura, J., Feng, K., Guo, D., & Huang, X., (2021). Active length of a continuous pipe or tunnel subjected to reverse faulting. Soil Dynamics and Earthquake Engineering, 148, 106825.

Zeng, G., Sawamura, Y., Geng, P., & Kishida, K., (2024). Analytical approach for determining the response of a tunnel structure crossing a reverse active fault. Tunnelling and Underground Space Technology, 146, 105590.